TISSUE ENGINEERING: Part A
Volume 19, Numbers 3 and 4, 2013

DOI: 10.1089/ten.tea.2012.0244

Integration of a Novel Injectable Nano Calcium Sulfate/Alginate Scaffold and *BMP2* Gene-Modified Mesenchymal Stem Cells for Bone Regeneration

Xiaoning He, DDS,[1,2] Rosemary Dziak, PhD,[1] Keya Mao, PhD,[3] Robert Genco, DDS, PhD,[1] Mark Swithart, PhD,[4] Chunyi Li, PhD,[1] and Shuying Yang, MD, PhD[1,5]

The repair of craniofacial bone defects is surgically challenging due to the complex anatomical structure of the craniofacial skeleton. Current strategies for bone tissue engineering using a preformed scaffold have not resulted in the expected clinical regeneration due to difficulty in seeding cells into the deep internal space of scaffold, and the inability to inject them in minimally invasive surgeries. In this study, we used the osteoconductive and mechanical properties of nano-scale calcium sulfate (nCS) and the biocompatibility of alginate to develop the injectable nCS/alginate (nCS/A) paste, and characterized the effect of this nCS/A paste loaded with bone morphogenetic protein 2 (*BMP2*) gene-modified rat mesenchymal stem cells (MSCs) on bone and blood vessel growth. Our results showed that the nCS/A paste was injectable under small injection forces. The mechanical properties of the nCS/A paste were increased with an increased proportion of alginate. MSCs maintained their viability after the injection, and MSCs and *BMP2* gene-modified MSCs in the injectable pastes remained viable, osteodifferentiated, and yielded high alkaline phosphatase activity. By testing the ability of this injectable paste and *BMP2*-gene-modified MSCs for the repair of critical-sized calvarial bone defects in a rat model, we found that *BMP2*-gene-modified MSCs in nCS/A (nCS/A+M/B2) showed robust osteogenic activity, which resulted in consistent bone bridging of the bone defects. The vessel density in nCS/A+M/B2 was significantly higher than that in the groups of blank control, nCS/A alone, and nCS/A mixed with MSCs (nCS/A+M). These results indicate that *BMP2* promotes MSCs-mediated bone formation and vascularization in nCS/A paste. Overall, the results demonstrated that the combination of injectable nCS/A paste and *BMP2*-gene-modified MSCs is a new and effective strategy for the repair of bone defects.

Introduction

Craniofacial destruction is devastating to patients with facial trauma, congenital deformities of the facial skeleton, and oral malignancies, because it leads to devastating effects on patients' quality of life. Current clinical therapies mainly rely on using grafting materials, including autografts, allografts, xenografts, or alloplasts. Although these therapies can restore certain craniofacial bone defects to a limited degree, they are far from ideal. For example, major concerns over the use of autografts include the need for a second site of surgery, insufficient supply, inadequate size and shape, and the morbidity associated with the donor site. Other grafts such as alloplasts, allografts, and xenografts have disadvantages such as carrying the risk of long-term foreign body reaction, pathogen transmission and immune rejection, multiple surgeries, facial scar formation, and limited new bone formation.[1–3] Hence, improved strategies are urgently needed to better treat critical-sized craniofacial bone defects with fewer surgeries, less scar formation and pain, and better aesthetic results.

One focus of craniofacial reconstructive research has been the use of tissue-engineered bone as a promising alternative to implant materials.[4] In bone tissue engineering, the scaffold plays a crucial role in defining the 3D anatomical shape and microenvironment for regenerative cells, favoring the regeneration of new bone, maintaining space, and preventing soft tissue prolapsed in the bony lesion. Traditional

[1]Department of Oral Biology, The State University of New York at Buffalo, Buffalo, New York.
[2]The 4th Affiliated Hospital of China Medical University, China Medical University, Shenyang, China.
[3]Department of Orthopaedic, Chinese People's Liberation Army General Hospital, Beijing, China.
[4]Department of Chemical and Biological Engineering, The State University of New York at Buffalo, Buffalo, New York.
[5]Developmental Genomics Group, New York State Center of Excellence in Bioinformatics and Life Sciences, University of Buffalo, The State University of New York, Buffalo, New York.

cell-based therapies have employed preformed scaffolds. These scaffolds have many drawbacks, including the requirement of an open surgery procedure[5] and machining the graft or carving the surgical site, which leads to increased bone loss, trauma, and surgical time;[6] the difficulty in seeding cells into the deep internal space of the scaffold; and the inability to inject in minimally invasive surgeries.[7] Facing the problems of irregular bone defects, injectable scaffolds are advantageous, because they can provide better performance in re-contoured craniofacial defects, incorporate various growth factors and cells, and do not require an open surgical procedure for placement.[7,8] Thus, they can shorten the surgical time, minimize the damage, and achieve rapid recovery. Several injectable hydrogel and polymer carriers have been shown to be meritorious for cell delivery.[7,9] However, these injectable carriers are not suitable for load-bearing repairs. Mechanical properties are important for the regeneration of load-bearing tissues such as the bone, to withstand stress to avoid scaffold fracture and maintain the structure to define the shape of the regenerated tissue.

Calcium sulfate (CS) is a crystalline structure. It is a biocompatible, bioactive, and biodegradable material.[10] CS has a compressive strength which is greater than that of cancellous bone. The application of CS includes the filling of cysts, bone cavities,[11,12] and segmental bone defects.[13] In previous reports, CS occupies a unique position in the injectable paste materials.[14–16] CS pastes can be easily injected percutaneously using a syringe and have been used in the treatment of periodontal disease, alveolar bone loss, and maxillary sinus augmentation,[17,18] and as an adjunct with other graft materials in guided tissue regeneration.[19] In recent years, significant progress has been made in various materials structured at the nano-scale.[20,21] Since nanoparticles have significant surface effects, size, and quantum effects, nanocomposites usually exhibit much better performance properties than do traditional materials. The improved relevant properties include enhanced strength, stiffness, improved transparency, increased scratch, abrasion, solvent and heat resistance, increased surface area, and decreased gas permeability.[22] Nano-calcium sulfate (nCS) particles in the range of 30–100 nm can enhance physical properties, such as high-surface area for growth factor adsorption, with the potential for controlling the rate of release of the adsorbed material, as well as superior mechanical strength for optimal osteoconductivity and resistance to fractures.[23] However, scaffolds made solely of these nano-scale particles have only nano-scale pores. These cannot provide space for cell migration and vascularization. Space for cells and blood vessels is one of the most important elements of scaffolds.[24,25] The addition of macro pores should not only enhance cell migration, but also help vascularization for oxygen and nutrient delivery, waste removal, and protein transport.[26,27]

Alginate is a natural anionic polysaccharide that is commonly obtained from brown seaweed. Due to its biocompatibility, low immunogenicity, mildness of gelation conditions, high hydrophilicity, biodegradability under normal physiological conditions, and low cost, purified alginate has been widely used in food and pharmaceutical industries and many biomedical therapeutic applications,[28–30] and for bone tissue engineering.[31–35] Alginate consists of poly-D-mannuronic acid (M) blocks, poly-L-guluronic acid (G) blocks, and alternating G/M blocks and forms stable hydrogels in the presence of certain divalent cations (i.e., Ca^{2+}) through the ionic interaction between the carboxylic acid group located on the polymer backbone and the chelating cation.[36,37] Alginate hydrogels cross-linked with calcium have the advantage of being injectable.[38] In addition, when a scaffold containing alginate is placed in the medium, there is uncontrolled degradation of ionically cross-linked alginate due to the loss of divalent cations.[39,40] This leads to the formation of pores inside the scaffold, which enhances cell migration.[41]

Although scaffolds provide templates for bone regeneration, biologic factors such as cells, growth factors, or genes are typically required to effectively repair challenging bone defects.[42] Mesenchymal stem cells (MSCs) are a population of multipotent, nonhematopoietic marrow-derived cells that are easily expanded in culture and differentiate into cells with an osteogenic (OS) phenotype.[43,44] Implantation of the MSCs has the potential to enhance healing of the bone.[45] Osteoinductive growth factors such as recombinant human bone morphogenetic protein-2 (rhBMP2) have demonstrated some clinical success for bone healing, but large sustainable doses[46,47] and the extremely high costs of manufacturing this glycoprotein[48] restrict its clinical applications. It has been proved that MSCs that are genetically engineered to express specific growth factors such as recombinant rhBMP2 have unique advantages for promoting bone regeneration because the gene expression in cells is stable, and this treatment modality is much less expensive than that using the recombinant protein.[49] Therefore, this study aims at developing an injectable, biodegradable, porous, and load-bearing nCS/alginate (nCS/A) delivery system for the implantation of *BMP2*-gene-modified MSCs to improve the treatment of critical-sized craniofacial bone defects. We developed and characterized the nCS/A paste delivery system, and analyzed the *in vitro* growth characteristic of *BMP2*-gene-modified MSCs in the nCS/A paste as well as the *in vivo* bone formation by the implantation of nCS/A paste with *BMP2*-gene-modified MSCs in a rat critical-sized calvarial defect.

Materials and Methods

Preparation and characterization of MSCs

See the Supplementary Materials and Methods (Supplementary Data are available online at www.liebertpub.com/tea).

Scaffold preparation

nCS was produced according to the method of Park *et al.*[23,50] Briefly, a cryo-vacuum process was used to convert hydrate CS into dihydrate nCS, which was then subjected to oven drying to produce hemihydrate nCS as previously described.[51] Sterilization was performed by glow discharge treatment. The injectable nCS/A pastes were formulated by varying the ratio of nCS and alginate. Briefly, alginate was dissolved in phosphate-buffered saline to prepare 15%, 10%, and 5% solution, and then, pH was adjusted to 7.2–7.4. About 127.5, 135, or 142.5 mg nCS powder was, respectively and correspondingly, mixed with 150 μL alginate in the ratios 85:15, 90:10, or 95:5. The total mass of nCS and alginate was 150 mg. After 2 min, a 25 μL cell suspension with 1×10^6

MSCs infected with Ad-*LacZ* or Ad-*BMP2* was added to the nCS/A paste to generate an injectable scaffold. Based on the ratio of alginate, they were named nCS/15%A, nCS/10%A, and nCS/5%A. All operations were performed at 4°C.

Scanning electron microscopy

MSCs mixed in nCS/A paste (nCS/15%A, nCS/10%A, and nCS/5%A) were cultured in a 48-well plate for 24 h and then fixed for scanning electron microscopic (SEM) analysis (See the Supplementary Materials and Methods).

Injectability testing

Injectability was determined as the mass of the paste extruded from the syringe divided by the total mass before injecting.[52,53] Each test was performed five times, and the average value was calculated. Please see the Supplementary Materials and Methods for details.

Mechanical testing

The nCS/15%A, nCS/10%A, and nCS/5%A pastes were, respectively, placed in $3\times4\times25$ mm molds; clamped between two glass slides[54]; then set in a humidor at 37°C for 4 h; and demolded and immersed in culture media (Modified Eagle's Medium alpha with 10% fetal bovine serum, 1× penicillin/streptomycin) at 37°C for 20 h before testing. A standard three-point flexural test (ASTM F 417-78) was used to fracture the specimens at a crosshead speed of 1 mm/min on a computer-controlled Universal Testing Machine (model 5500R). The flexural strength was calculated by $S=3La/(2bh^2)$, where L is the maximum load on the load-displacement curve, a is the span, b is the specimen width, and h is the specimen thickness.[55,56]

BMP2 gene expression[57]

See the Supplementary Materials and Methods.

MTS cell viability assay

The cell viability was assayed using MTS cell viability assay kit (Promega). Briefly, the cultured MSCs were randomly divided into three groups: nCS seeding group: MSCs were seeded on an nCS/10%A scaffold; nCS mixture group: MSCs were mixed with nCS/10%A paste; and plate group: MSCs were directly plated in a 96-well plate. There were five wells for each time point and each group. The cells in each group were then induced with OS medium (culture media supplemented with 50 μg/mL ascorbic acid, 10^{-8} M dexamethasone, and 10 mM sodium β-gylcerol-phosphate) for 24, 48, and 72 h, respectively, and then, the cell viability at different time points was analyzed by using the MTS cell viability assay kit. Briefly, 20 μL MTS assay solution was added to the cultured cells with 100 μL culture media, and incubated at 37°C for 3 h. Then, the supernatants were transferred in a 96-well microtiter plate for measuring the OD value at 490 nm using a microplate reader.

Alkaline phosphatase activity assay

MSCs were infected with Ad-*lacZ* or Ad-*BMP2* for 24 h. Then, the cells were seeded on or mixed with nCS/10%A paste and induced with OS media for 7 days. Alkaline phosphatase (ALP) activity was determined by using an ALP assay kit in keeping with the manufacturer's instructions (Sigma). ALP activity was normalized with the value of DNA content and expressed as nmol of p-nitrophenol produced per minute per milligram of total DNA.[58] DNA concentration was measured according to the method of Schneider *et al*.[59]

Osteoblast cell marker gene expression

See the Supplementary Materials and Methods.

Rat critical-sized calvarial bone defect model

Twenty-four male Sprague Dawley (SD) rats at 8 weeks old were used in this study. The *in vivo* experimental protocol was reviewed and approved by the University at Buffalo Animal Care and Use Committee. Please see the Supplementary Materials and Methods for general anesthesia, surgery, and postoperational care procedures. The animals were divided into four groups: group 1, blank control; group 2, nCS/A; group 3, nCS/A + MSC (nCA/A + M); and group 4 nCS/A + *BMP2*-gene-modified MSC (nCS/A + M/B2). At the end of the 7-week period, the animals were euthanized using CO_2, and all implants were harvested for a further analysis.

Analysis of in vivo *bone formation*

Bone density measurements (BMD, g/cm^2) of all implants from the rats (six rats per group) were performed using a LUNAR PIXImus bone densitometer. LUNAR PIXImus software was used to analyze the scanned data. On the computerized scan plots, five regions of interest per implant were selected to measure the BMD of the defect area, and the average values were taken as the final result per implant. This allowed BMD measurement in close relation to the bone regeneration area by excluding pixels by the software. For histological analysis, half specimens (half implant) per group were decalcified and cut into 5 μm sections. The sections were then stained with hematoxylin and eosin. The ratio of the bone area in the implants against the total implant tissue of section was quantified using NIH Image J software and defined as the percentage of bone volume in the implant/total volume of the implant. The other half specimens were used for ALP activity analysis as previously described.

Analysis of blood vessel ingrowth

Paraffin-embedded decalcified bone sections were processed for immunohistochemistry staining for Von Willebrand factor (vWF).[60] Primary antibody (goat vWF antibody) was diluted 1:300 (Abcam), and secondary rabbit anti-goat antibody conjugated to horseradish peroxidase was diluted 1:500 in 1% bovine serum albumin. Blood vessels, indicated by vWF staining, were counted manually at 10× magnification in the total implant area and normalized to the implant area with the use of Image J software.

Statistical analysis

Statistical analysis was performed using SPSS-17.0 software. Where indicated, experimental data were reported as mean ± standard deviation of triplicate independent samples.

Data were analyzed using Student's *t*-test and one-way analysis of variance, and Tukey's HSD test was applied as a *post hoc* test if statistical significance was determined. A value of $p \leq 0.05$ was considered statistically significant.

Results

Characterization of MSCs

A number of surface proteins have been used to enrich rat MSCs, including CD29, CD44, CD90, CD73, CD105, CD271, and Stro-I.[61,62] In our study, we used CD44 and CD90 as positive markers to enrich MSCs. The hematopoietic stem cells (HSC) marker CD34 and endothelial progenitor cell (EPC) marker CD31 was used to confirm that the MSCs were depleted of HSCs and EPCs.[63] As shown in Figure 1A, more than 96% of the cells expressed CD90 (96.2%) and CD44 (97%). In contrast, there were scarcely CD31-positive endothelial cells (4.5%) or CD34-positive immature hematopoietic cells (7.7%). Immunostaining results showed that MSCs were positive for CD44 and CD90 (Fig. 1B). In addition, MSCs could be successfully differentiated into three cell lineages—osteoblasts, chondrocytes, and adipocytes (Fig. 1C).

Injectable and porous nCS/A delivery system

Dissolution tests showed that the integrity of nCS/A scaffolds with 50% and 30% alginate was completely lost after 48 h, nCS/15%A partially maintained their shape, but nCS/10%A and nCS/5%A completely maintained their shape (Supplementary Fig. S1A). Therefore, we chose nCS/5%A, nCS/10%A, and nCS/15%A for further studies. Injectability analysis showed that all three kinds of pastes were readily extruded at relatively small injection forces. Compared with nCS alone, the injection forces for nCS with alginate were higher in an alginate dose-dependent pattern ($p < 0.05$) (Fig. 2A). Mechanical property tests showed an increase in strength for all loadings of nCS with different ratios of alginate relative to nCS alone ($p < 0.05$) (Fig. 2B). We found that the MSCs cell viability in nCS/10%A was better than nCS/5%A and nCS/15%A (see Supplementary Fig. S1B). Moreover, SEM analysis showed that the average pore diameter in the nCS/10%A scaffold was 70–80 μm (Fig. 2C, D), and the cells attached on the nCS/10%A scaffold (Fig. 2E). Combining these observations, we selected nCS/10%A as an optimal concentration for further experiments.

nCS/A paste and BMP2 gene modification promotes MSCs osteoblast differentiation

To determine whether mixing MSCs with injectable nCS/A paste affects MSCs viability and proliferation, an MTS cell viability assay was performed in three groups—seeding, mixing, and plating. The results showed no significant differences in cell viability among three groups, indicating that mixing MSCs with injectable nCS/A paste does not affect MSCs viability and proliferation, and, hence, nCS/10%A paste is likely not toxic (Fig. 3A). To investigate the safety of *Ad-BMP2* to the MSCs, cell viability and mineralization were analyzed by using different titers of *Ad-BMP2* to infect cells. The results showed that the cells infected with the multiplicity of infection (MOI) 100 and 50 showed normal cell growth and stronger cell mineralization compared with other groups, indicating that *Ad-BMP2* at MOI 100 and 50 had no toxicity to the cells (see Supplementary Fig. S2A, B). To trace the expression level of BMP2 in *BMP2* gene-modified MSCs, the BMP2 levels in the culture media were measured by ELISA Kit. The results showed that the BMP2 level reached a peak at day 4, then slowly decreased over 14 days, and finally rapidly dropped down to the control level (Fig. 3B) at day 21. At day 7 after OS media induction, ALP activity in the *BMP2*-gene-modified MSCs group (nCS/A+M/B2) was about 2.4-fold higher than that in MSCs group

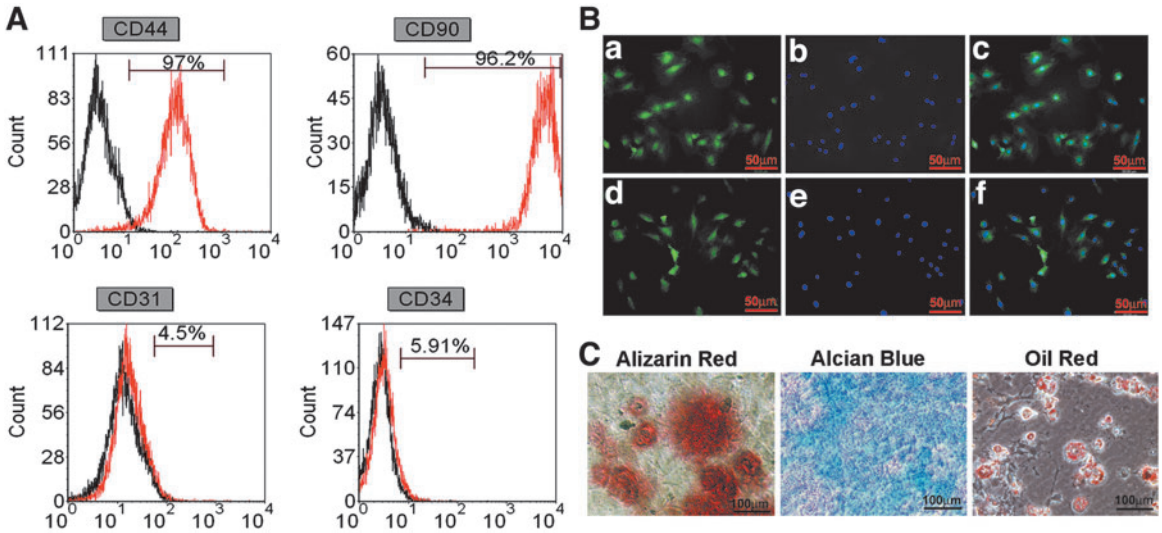

FIG. 1. Phenotype identification of mesenchymal stem cells (MSCs). **(A)** Flow cytometry analysis. The black open histograms show isotype-matched control. The red open histograms indicate cells stained with markers of undifferentiated MSCs. **(B)** Immunostaining for MSCs marker genes CD90 **(a)** MSCs positive for CD90; **(b)** 4′,6-diamidino-2-phenylindole (DAPI); **(c)**, merged image of **(a)** and **(b)** and CD44 **(d)**, MSCs positive for CD44; **(e)** DAPI; **(f)** merged image of **(d)** and **(e)**. **(C)** Alizarin red S staining: mineral deposition by MSCs cultured in an osteogenic medium, indicating osteogenesis. Alcian Blue staining: proteoglycans produced by MSCs cultured in a chondrogenic medium, indicating chondrogenesis. Oil red O staining: fat globules seen in MSCs cultured in an adipogenic medium, indicating differentiation into adipocytes. Color images available online at www.liebertpub.com/tea

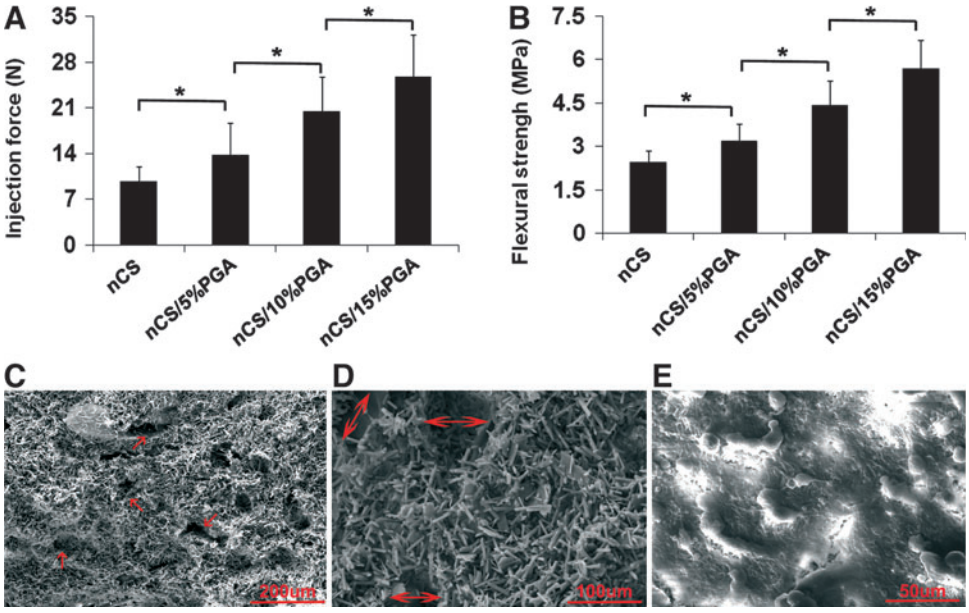

FIG. 2. Properties of injectable nano-calcium sulfate/alginate (nCS/A) pastes. **(A)** Injection force versus syringe plunger displacement for nCS/A paste. **(B)** Mechanical properties of nCS/A composite. **(A, B)** Error bars represent mean ± standard deviation for $N = 8$. *$p < 0.05$. **(C)** Scanning electron microscopic (SEM) view of injectable nCS/10%A pastes at a magnification of 200×. Red arrows: pores. **(D)** SEM view of injectable nCS/10%A pastes at a magnification of 500×. Red arrows: pore diameter. **(E)** SEM view of MSCs cultured in nCS/10%A pastes at a magnification of 1000×. Color images available online at www.liebertpub.com/tea

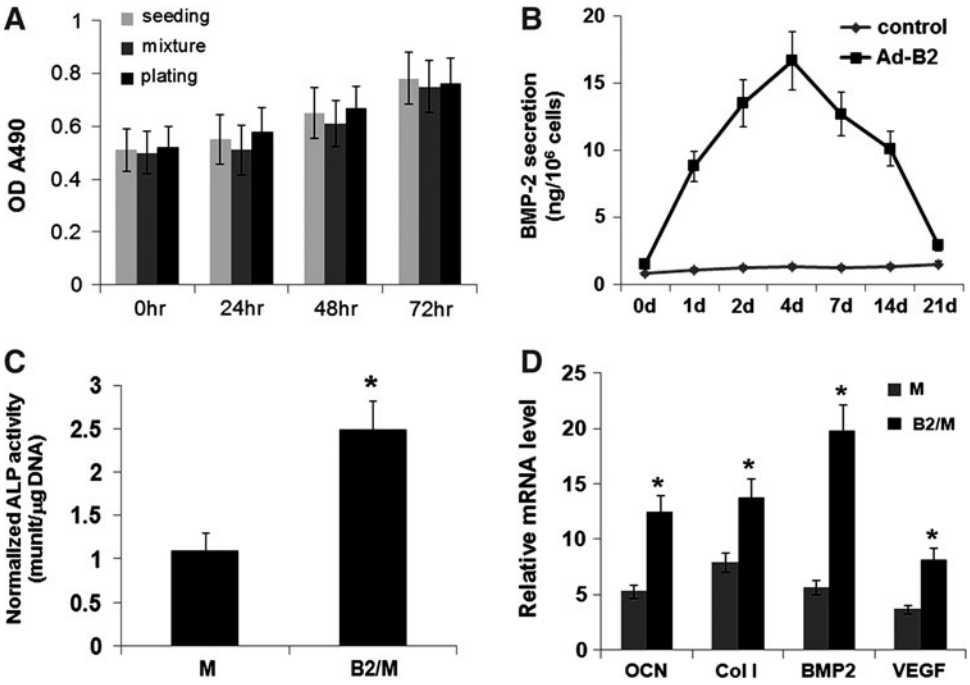

FIG. 3. Osteoblastic differentiation of bone morphogenetic protein 2 (*BMP2*) gene-modified MSCs in injectable nCS/A paste. **(A)** MTS cell viability assay. The cell number was 5×10^4 per scaffold for the three groups. Data represent the mean ± standard deviation for $N = 8$. $p > 0.05$: mixture group versus seeding or plate groups at time points of 24, 48 and 72 h. **(B)** Duration of BMP2 secretion. Adenovirus-mediated gene transfers led to the secretion of BMP2 for about 21 days after transfection. **(C)** Alkaline phosphatase (ALP) activity in *BMP2*-gene-modified MSCs group was about 2.5-fold higher than that in MSCs group. $N = 6$. *$p < 0.001$. **(D)** quantitative reverse transcriptase polymerase chain reaction analysis of osteoblast marker genes, result showed that the MSC with injectable nCS/10%A dramatically increased osteocalcin (*OCN*), type I collagen (*Col I*), *BMP2*, and vascular endothelial growth factor (*VEGF*) gene expression. Data represent the mean ± standard deviation of $N = 6$ samples. *$p < 0.001$.

(nCS/A+M) (Fig. 3C). Moreover, quantitative reverse transcriptase–polymerase chain reaction showed that *osteocalcin* (*OCN*), *type I collagen* (*Col I*), *BMP2*, and *vascular endothelial growth factor* (*VEGF*) gene expression dramatically increased in the nCS/A+M/B2 group compared with that in the nCS/A+M group (Fig. 3D). These data indicate that *BMP2* is a strong enhancer for bone regeneration mediated by the injectable nCS/A with MSCs construct.

Injectable nCS/A delivery system with gene-modified MSCs promotes bone regeneration

To evaluate the potential of the construct of injectable nCS delivery system and *BMP2* gene-modified MSCs for bone regeneration *in vivo*, an 8-mm defect was created in the calvarial bones of SD rats. At 7 weeks after implantation, Faxitron x-ray (Fig. 4A) results showed that the *BMP2*-gene-modified

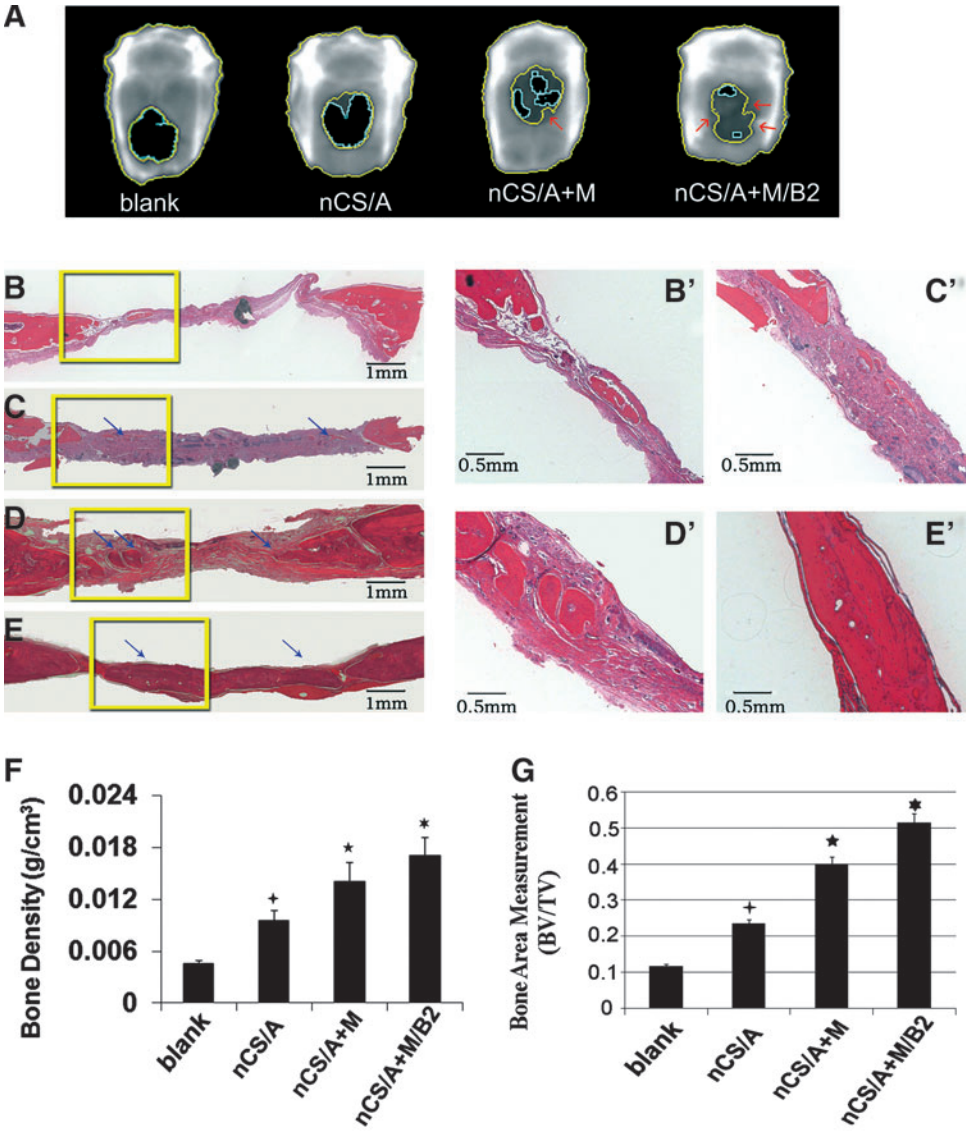

FIG. 4. *BMP2*-gene-modified MSCs in injectable nCS/A paste enhances bone regeneration in the rat critical-sized calvarial defect model. **(A)** Image of calvarial bone from LUNAR PIXImus system, 7 weeks after surgery. The bone regeneration areas were labeled by different colors. Black area circled with a light blue open line is the low-density area (fibrous tissue). The dark gray area between the light blue line and the inside yellow line is the higher bone density area, the area between two yellow lines is considered the highest bone density area, and the density in this area is close to normal bone tissue. The arrows show the normal bone in the bone defect region. **(B–E, B′–E′)**. Hematoxylin and eosin staining. Coronal sections through the midline of defects are shown. Margins of the original 8.0-mm trephine defect are shown. **(B–E)**: lower magnification, Bar = 1 mm; **(B′–E′)**: higher magnification, Bar = 0.5 mm. The arrows show newly formed bone. **(B, B′)**: Blank; **(C, C′)**: nCS/A; **(D, D′)**: nCS/A+M; **(E, E′)**: nCS/A+M/B2. **(F)**. Quantitative analysis of bone density from **(A)**. $N = 6$, $^*p < 0.05$: nCS/M/B2 versus three other groups. $^*p < 0.05$: nCS/M versus nCS or blank. $^*p < 0.05$: nCS versus blank. **(G)** Quantitative analysis of bone area in implanted region from **(B–E)** BV, bone area in the implant; TV, total implant area. $N = 6$, $^*p < 0.05$: nCS/M/B2 versus three other groups. $^*p < 0.05$: nCS/M versus nCS or blank. $^*p < 0.05$: nCS versus blank. Color images available online at www.liebertpub.com/tea

MSCs group (nCS/A+M/B2) exhibited nearly complete closure of bony defects with much more newly formed bone with normal BMD compared with other groups. *AdLacZ*-transduced MSCs group (nCS/A+M) also showed more area with higher BMD than the blank control and nCS/A groups. nCS/A group showed a small amount of new bone, but had no normal BMD area ($p<0.05$). A quantitative analysis of BMD (Fig. 4F) showed that the BMD in the nCS/A+M/B2 group was significantly higher than that in the other groups. Without *BMP2* gene transduction, the BMD in nCS/M was also significantly higher than that in nCS/A and the control (blank) groups; however, it was much lower than that in the nCS/A + M/B2 group. Notably, the nCS/A group also showed significantly higher BMD compared with the blank group. Consistent with the x-ray BMD result, histological analysis (Fig. 4B–E, B′-E′) showed that there was a larger amount of new bone formed in nCS/A+M/B2 and nCS/A+M groups (Fig. 4D, D′ E, E′). Compared with the nCS/A+M group, which induced partial bone defect healing, the nCS/A+M/B2 group exhibited robust OS activity, with complete coverage of defects with newly formed bone in most samples. In addition, there were also small regions of osteoid matrix within the interior of the implants in the nCS/A group (Fig. 4C, C′) relative to the blank control (Fig. 4B, B′). These results indicate that nCS/A paste can stimulate new bone formation. Furthermore, a histomorphometric analysis of histological slides also showed a significantly larger bone area within the nCS/A+M/B2 implant when compared with the other three groups (Fig. 4G).

Injectable nCS/A delivery system with BMP2-gene-modified MSCs promotes blood vessel growth

vWF is a glycoprotein that is synthesized in endothelial cells and megakaryocytes and presents in large quantities in subendothelial matrices such as vessel basement membranes.[64] Due to this, vWF has been considered a useful marker for detecting blood vessels by immunohistochemistry.[65] To determine the effects of injectable nCS/A delivery system with *BMP2*-gene-modified MSCs on blood vessel ingrowth in a bone defect model, the densities of blood vessels present in the nCS/A+M/B2 and nCS/A+M groups were measured by histological sections staining for vWF. The results showed that nCS/A+M/B2 implant areas displayed a higher density of blood vessels interspersed throughout the implant region compared with that in the nCS/A+M implant region (Fig. 5A). Quantification of blood vessel area throughout the total implant area confirmed that nCS/A+M/B2 implants had a significantly higher blood vessel density than nCS/A+M (Fig. 5B). The results just cited indicate that *BMP2*-gene-modified MSCs in nCS/A paste can induce angiogenesis and lead to more bone regeneration within the defect area.

Discussion

To improve healing of critical-sized defects, to date, a major barrier is the lack of sufficient integration of biomaterial design and engineered cells such as stem cells to promote bone regeneration. Although many studies use MSCs and scaffolds of calcium-based minerals,[66–68] this was the first that evaluated the combination of *BMP2*-gene-modified MSCs with an injectable and porous nCS/A paste. The results of this study demonstrated the importance and efficiency of this injectable system in bone regeneration, and highlighted the potential utility of this construct for bone repair and regeneration.

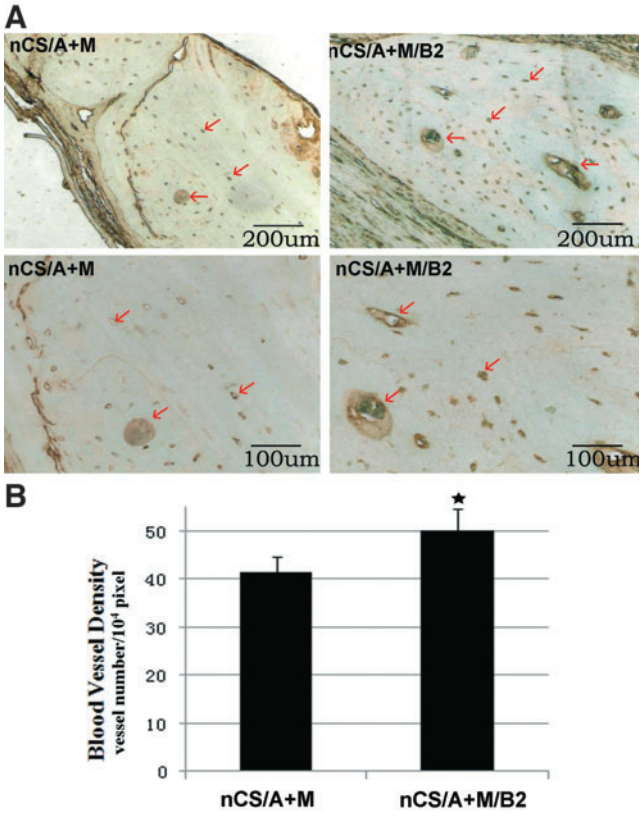

FIG. 5. *BMP2*-gene-modified MSCs in injectable nCS/A paste promotes angiogenesis. **(A)** Immunostaining of endothelial cell marker—Von Willebrand factor (vWF). Brown color in new bone regions indicate positive staining for blood vessels. The arrows show the blood vessel positive for vWF in the bone defect region. Top panel: lower magnification, bar = 200 μm; bottom panels: higher magnification, bar = 100 μm. **(B)** Quantitative analysis of blood vessel density from **(A)**. $N=6$, $^*p<0.05$: nCS/M/E/B2 versus nCS/M. Color images available online at www.liebertpub.com/tea

In previous studies, beta-tricalcium phosphate and hydroxyapatite composites were used as bone repair materials for delivering MSCs or growth factors, and have been proved to have good OS characteristics.[69,70] However, these delivery constructs lack good plasticity, and the cellular implantation procedure is complicated due to problems such as brittleness, poor mold ability, and inappropriate rate of biodegradability for the respective cells to multiply.[25,71] Recently, Yamada *et al.*[72] used a combination of platelet-rich plasma as an injectable scaffold with MSCs to increase osteogenesis and found a progressive, complete resorption of the scaffold and enhanced new bone formation. However, similar to injectable hydrogel and polymer carriers, one downside to this scaffold is that the inadequate mechanical strength easily causes the deformation under load, which restricts its application for the critical-sized bone defect, especially for the craniofacial bone defect.[72] Compared with those materials and/or scaffolds, the hemihydrate of CS is a

highly biocompatible, osteoconductive, and biodegradable material that is one of the simplest synthetic bone-like fillers[17,73] and injectable paste material.[14–16] In this study, by extending the work presented in Park *et al.*,[23] we combined nCS and alginate and developed a novel injectable and porous nCS/A system. We used nCS as a base carrier to increase surface area for stem cells and soft tissue attachment, and used alginate to produce pores and adjust the strength of the paste. Our results showed that the presence of alginate increased the strength of the nCS material, but did not significantly affect the cell viability. Consistent with this finding, Bron *et al.*[74] also found that the concentration of alginate in the range used here provides higher stiffness in the scaffolds, but does not affect cell viability. Although the most commonly-used concentration of alginate for drug and cell delivery is between 1% and 3% (m/v%),[75,76] in tissue-engineering application, more and more studies have used higher concentrations to increase mechanical strength and generate pores by using different strategies, and found that higher concentrations of alginate do not affect cell viability.[74,77,78] Both the *in vivo* and *in vitro* results presented here demonstrate that the nCS/10%A composition not only is biocompatible and has proper biodegradability, but also promotes OS differentiation of stem cells without decreasing cell viability.

Previous studies have shown that bone ingrowth into porous systems with different pore sizes and the diameter of interconnecting pores determine the quality of tissue growing into the porosity space.[79–82] The most optimal pore size for mineralized bone ingrowth still seems to be a controversial topic. For example, Hulbert *et al*.[83] concluded that the interconnections of the porosity should be larger than 100 μm for regenerating mineralized bone. In contrast, Bobyn *et al.*[84] found that effective bone ingrowth into porous space can happen in the scaffold with pore sizes down to 50 μm, whereas the Itala group[79] showed that there is no threshold value for new bone ingrowth in pore sizes ranging from 50 to 125 μm under nonload-bearing conditions. Our results showed that the average pore diameter of micro-pores generated in the nCS/10%A injectable was 70–80 μm. Our *in vitro* and *in vivo* studies further showed that 70–80 μm of nCS/10%A could lead to effective cell proliferation and bone ingrowth, suggesting that an nCS/10%A scaffold with 70–80 μm pore size is suitable for bone ingrowth.

BMPs are potent morphogens with a strong OS potential.[85] rhBMP2 has obtained U.S. Food and Drug Administration approval for human applications to stimulate spinal fusion and repair nonunion long bone defects.[86–88] However, these trials demonstrated some disadvantages such as difficulty in retaining BMPs in a biomaterial matrix, high BMP loading requirements, and high cost.[89] MSCs that are genetically engineered to express specific growth factors have unique advantages for promoting bone regeneration due to their relatively stable expression of growth factors and them being less expensive than using the recombinant proteins.[90,91] In this study, by injecting nCS/10%A paste mixed with *BMP2*-gene-modified MSCs (nCS/A+M/B2) into well-established critical-sized rat calvarial bone defects,[92] we found that the BMD was much higher than that in other groups and exhibited nearly complete closure of bony defects in a short time (7 weeks). Histological analysis complemented the BMD result. All defects in this group were almost covered with mineralized bone tissue. These results demonstrated that injectable nCS/A paste is a biodegradable and biocompatible scaffold, and genetically engineered expression of *BMP2* in MSCs in nCS/10%A paste can provide an even more effective approach for repair of a critical-sized bone defect.[93] Notably, the critical-sized defects were repaired much better in the MSCs-containing groups compared with the group without MSCs (see Fig. 5), and exhibited no sign of rejection in all groups, indicating that at least most of the implanted allogeneic MSCs maintained their viability and had no apparent immunorejection of the host. This conclusion was supported by some previous findings. For example, Li *et al.*[94] found that there is no immunological rejection and graft versus host disease by intravenously injecting green fluorescent protein-labeled allogeneic MSCs into rabbits. Saito *et al.*[95] found that the rats have immunological tolerance to mouse MSCs. Devine *et al.*[96] reported that human MSCs persist after infusion *in utero* to fetal sheep. Inoue *et al.*[97] found that MSCs express very low levels of immunogenic class Ia and II molecules from the major histocompatibility complex and that MSCs lack immunogenic antigens. In addition, the results of this study support the concept that BMP2 can enhance angiogenesis and bone regeneration.[98,99] Localized and sustained BMP2 delivery from MSCs significantly increased the expression of osteoblast marker genes and *VEGF* and promoted blood-vessel density and bone formation in the bone defect area. Hence, the effects of BMP2 delivery in MSCs observed in this study corroborate the previous work that highlights the importance of BMP2 and MSCs in angiogenesis and bone healing.

In conclusion, this study provides the first evidence of support that this novel injectable nCS/A paste can stimulate bone formation and is an efficient vehicle for stem cells to promote new bone formation. The combination of the nCS/A paste with *BMP2*-gene-modified MSCs can dramatically enhance new bone formation and angiogenesis, and lead to a nearly complete repair of critical-sized calvarial bone defects. On the basis of the data presented here, it appears that this system can be useful not only in critical-sized bone defect, but also in the filling of defects with limited accessibility or narrow cavities such as in periodontal bone repair. Its use in minimally invasive techniques, such as *in situ* fracture fixation and percutaneous vertebroplasty to fill the lesions and strengthen osteoporotic bone, is another area to further pursuit.

Acknowledgments

The authors thank David Hadbawnik for a critical reading of the article, and Dr. Wade J. Sigurdson, the director of the Flow Cytometry Facility at the School of Medicine and Biomedical Sciences, University at Buffalo, for assistance with the flow cytometry assay. They thank Dr. Neoyuli Hanaki for technical assistance with making a critical-sized calvarial bone defect model. This work was supported by a National Institute of Health grants AR055678 (S. Yang) and AR061052 (S. Yang).

Disclosure Statement

No competing financial interests exist.

References

1. Bowers, G.M., Chadroff, B., Carnevale, R., Mellonig, J., Corio, R., Emerson, J., *et al.* Histologic evaluation of new

attachment apparatus formation in humans. Part III. J Periodontol **60,** 683, 1989.
2. Laurell, L., Gottlow, J., Zybutz, M., and Persson, R. Treatment of intrabony defects by different surgical procedures. A literature review. J Periodontol **69,** 303, 1998.
3. Samstein, B., and Platt, J.L. Physiologic and immunologic hurdles to xenotransplantation. J Am Soc Nephrol **12,** 182, 2001.
4. Zuk, P.A. Tissue engineering craniofacial defects with adult stem cells? Are we ready yet? Pediatr Res **63,** 478, 2008.
5. Li, Z., Ramay, H.R., Hauch, K.D., Xiao, D., and Zhang, M. Chitosan-alginate hybrid scaffolds for bone tissue engineering. Biomaterials **26,** 3919, 2005.
6. Laurencin, C.T., Ambrosio, A.M., Borden, M.D., and Cooper, J.A., Jr. Tissue engineering: orthopedic applications. Annu Rev Biomed Eng **1,** 19, 1999.
7. Kretlow, J.D., Young, S., Klouda, L., Wong, M., and Mikos, A.G. Injectable biomaterials for regenerating complex craniofacial tissues. Adv Mater **21,** 3368, 2009.
8. Xu, H.H., Weir, M.D., and Simon, C.G. Injectable and strong nano-apatite scaffolds for cell/growth factor delivery and bone regeneration. Dent Mater **24,** 1212, 2008.
9. Drury, J.L., and Mooney, D.J. Hydrogels for tissue engineering: scaffold design variables and applications. Biomaterials **24,** 4337, 2003.
10. Peters, C.L., Hines, J.L., Bachus, K.N., Craig, M.A., and Bloebaum, R.D. Biological effects of calcium sulfate as a bone graft substitute in ovine metaphyseal defects. J Biomed Mater Res Part A **76,** 456, 2006.
11. Maeda, S.T., Bramane, C.M., Taga, R., Garcia, R.B., de Moraes, I.G., and Bernadineli, N. Evaluation of surgical cavities filled with three types of calcium sulfate. J Appl Oral Sci **15,** 416, 2007.
12. Kim, J.H., Oh, J.H., Han, I., Kim, H.S., and Chung, S.W. Grafting using injectable calcium sulfate in bone tumor surgery: comparison with demineralized bone matrix-based grafting. Clin Orthop Surg **3,** 191, 2011.
13. Qi, Y., Wang, Y., Yan, W., Li, H., Shi, Z., and Pan, Z. Combined mesenchymal stem cell sheets and rhBMP-2-releasing calcium-sulfate-rhBMP-2 scaffolds for segmental bone tissue engineering. Cell Transplant **21,** 693, 2012.
14. Zhao, W., Chang, J., and Zhai, W. Self-setting properties and *in vitro* bioactivity of $Ca_3SiO_5/CaSO_4{\cdot}1/2H_2O$ composite cement. J Biomed Mater Res A **85,** 336, 2008.
15. Chen, Z., Liu, H., Liu, X., and Cui, F.Z. Injectable calcium sulfate/mineralized collagen-based bone repair materials with regulable self-setting properties. J Biomed Mater Res A **99,** 554, 2011.
16. Cho, B.C., Park, J.W., Baik, B.S., and Kim, I.S. Clinical application of injectable calcium sulfate on early bony consolidation in distraction osteogenesis for the treatment of craniofacial microsomia. J Craniofac Surg **13,** 465; discussion 75, 2002.
17. Murashima, Y., Yoshikawa, G., Wadachi, R., Sawada, N., and Suda, H. Calcium sulphate as a bone substitute for various osseous defects in conjunction with apicectomy. Int Endod J **35,** 768, 2002.
18. Sukumar, S., Drizhal, I., Paulusova, V., and Bukac, J. Surgical treatment of periodontal intrabony defects with calcium sulphate in combination with beta-tricalcium phosphate: clinical observations two years post-surgery. Acta Medica (Hradec Kralove) **54,** 13, 2011.
19. Pecora, G., Andreana, S., Margarone, J.E., 3rd, Covani, U., and Sottosanti, J.S. Bone regeneration with a calcium sulfate barrier. Oral Surg Oral Med Oral Pathol Oral Radiol Endod **84,** 424, 1997.
20. Zhang, S. Fabrication of novel biomaterials through molecular self-assembly. Nat Biotechnol **21,** 1171, 2003.
21. Stupp, S.I., and Braun, P.V. Molecular manipulation of microstructures: biomaterials, ceramics, and semiconductors. Science **277,** 1242, 1997.
22. Kong, L.X., Peng, Z., Li, S.D., and Bartold, P.M. Nanotechnology and its role in the management of periodontal diseases. Periodontol 2000 **40,** 184, 2006.
23. Park, Y.B., Mohan, K., Al-Sanousi, A., Almaghrabi, B., Genco, R.J., Swihart, M.T., *et al.* Synthesis and characterization of nanocrystalline calcium sulfate for use in osseous regeneration. Biomed Mater **6,** 055007, 2011.
24. Mastrogiacomo, M., Muraglia, A., Komlev, V., Peyrin, F., Rustichelli, F., Crovace, A., *et al.* Tissue engineering of bone: search for a better scaffold. Orthod Craniofac Res **8,** 277, 2005.
25. Hollister, S.J. Porous scaffold design for tissue engineering. Nat Mater **4,** 518, 2005.
26. Lin, H.R., and Yeh, Y.J. Porous alginate/hydroxyapatite composite scaffolds for bone tissue engineering: preparation, characterization, and *in vitro* studies. J Biomed Mater Res B Appl Biomater **71,** 52, 2004.
27. Grandi, C., Di Liddo, R., Paganin, P., Lora, S., Dalzoppo, D., Feltrin, G., *et al.* Porous alginate/poly(epsilon-caprolactone) scaffolds: preparation, characterization and *in vitro* biological activity. Int J Mol Med **27,** 455, 2011.
28. Shang, Q., Wang, Z., Liu, W., Shi, Y., Cui, L., and Cao, Y. Tissue-engineered bone repair of sheep cranial defects with autologous bone marrow stromal cells. J Craniofac Surg **12,** 586; discussion 94, 2001.
29. Chang, S.C., Rowley, J.A., Tobias, G., Genes, N.G., Roy, A.K., Mooney, D.J., *et al.* Injection molding of chondrocyte/alginate constructs in the shape of facial implants. J Biomed Mater Res **55,** 503, 2001.
30. Thomas, S. Alginate dressings in surgery and wound management—Part 1. J Wound Care **9,** 56, 2000.
31. Smidsrod, O., and Skjak-Braek, G. Alginate as immobilization matrix for cells. Trends Biotechnol **8,** 71, 1990.
32. Matthew, I.R., Browne, R.M., Frame, J.W., and Millar, B.G. Subperiosteal behaviour of alginate and cellulose wound dressing materials. Biomaterials **16,** 275, 1995.
33. Wang, L., Shelton, R.M., Cooper, P.R., Lawson, M., Triffitt, J.T., and Barralet, J.E. Evaluation of sodium alginate for bone marrow cell tissue engineering. Biomaterials **24,** 3475, 2003.
34. Dobratz, E.J., Kim, S.W., Voglewede, A., and Park, S.S. Injectable cartilage: using alginate and human chondrocytes. Arch Facial Plast Surg **11,** 40, 2009.
35. Oest, M.E., Dupont, K.M., Kong, H.J., Mooney, D.J., and Guldberg, R.E. Quantitative assessment of scaffold and growth factor-mediated repair of critically sized bone defects. J Orthop Res **25,** 941, 2007.
36. Grant, G.T., Morris, E.R., Rees, D.A., Smith, P.J.C., and Thom, D. Biological interactions between polysaccharides and divalent cations - egg-box model. FEBS Lett **32,** 195, 1973.
37. Stokke, B.T., Smidsrod, O., Bruheim, P., and Skjakbraek, G. Distribution of uronate residues in alginate chains in relation to alginate gelling properties. Macromolecules **24,** 4637, 1991.
38. Lee, G.S., Park, J.H., Shin, U.S., and Kim, H.W. Direct deposited porous scaffolds of calcium phosphate cement with

alginate for drug delivery and bone tissue engineering. Acta Biomater **7,** 3178, 2011.
39. Wee, S., and Gombotz, W.R. Protein release from alginate matrices. Adv Drug Deliv Rev **31,** 267, 1998.
40. Tan, R., Feng, Q., Jin, H., Li, J., Yu, X., She, Z., *et al.* Structure and biocompatibility of an injectable bone regeneration composite. J Biomater Sci Polym Ed **22,** 1861, 2011.
41. Hyland, L.L., Taraban, M.B., Hammouda, B., and Bruce Yu, Y. Mutually reinforced multicomponent polysaccharide networks. Biopolymers **95,** 840, 2011.
42. Bruder, S.P., Kraus, K.H., Goldberg, V.M., and Kadiyala, S. The effect of implants loaded with autologous mesenchymal stem cells on the healing of canine segmental bone defects. J Bone Joint Surg Am **80,** 985, 1998.
43. Pittenger, M.F., Mackay, A.M., Beck, S.C., Jaiswal, R.K., Douglas, R., Mosca, J.D., *et al.* Multilineage potential of adult human mesenchymal stem cells. Science **284,** 143, 1999.
44. Muschler, G.F., Nakamoto, C., and Griffith, L.G. Engineering principles of clinical cell-based tissue engineering. J Bone Joint Surg Am **86-A,** 1541, 2004.
45. Wang, C., Wang, Z., Li, A., Bai, F., Lu, J., Xu, S., *et al.* Repair of segmental bone-defect of goat's tibia using a dynamic perfusion culture tissue engineering bone. J Biomed Mater Res A **92,** 1145, 2010.
46. Azad, V., Breitbart, E., Al-Zube, L., Yeh, S., O'Connor, J.P., and Lin, S.S. rhBMP-2 enhances the bone healing response in a diabetic rat segmental defect model. J Orthop Trauma **23,** 267, 2009.
47. Jones, A.L., Bucholz, R.W., Bosse, M.J., Mirza, S.K., Lyon, T.R., Webb, L.X., *et al.* Recombinant human BMP-2 and allograft compared with autogenous bone graft for reconstruction of diaphyseal tibial fractures with cortical defects. A randomized, controlled trial. J Bone Joint Surg Am **88,** 1431, 2006.
48. Gautschi, O.P., Frey, S.P., and Zellweger, R. Bone morphogenetic proteins in clinical applications. ANZ J Surg **77,** 626, 2007.
49. Yue, B., Lu, B., Dai, K.R., Zhang, X.L., Yu, C.F., Lou, J.R., *et al.* BMP2 gene therapy on the repair of bone defects of aged rats. Calcif Tissue Int **77,** 395, 2005.
50. Park, Y., Dziak, R., Genco, R., Swihart, M.T., and Periopanayagam, H. Calcium Sulfate Based Nanoparticles. US Patent: US7767226.
51. Salvadori, B., Capitani, G., Mellini, M., and Dei, L. A novel method to prepare inorganic water-soluble nanocrystals. J Colloid Interface Sci **298,** 487, 2006.
52. Khairoun, I., Boltong, M.G., Driessens, F.C., and Planell, J.A. Some factors controlling the injectability of calcium phosphate bone cements. J Mater Sci Mater Med **9,** 425, 1998.
53. Ginebra, M.P., Rilliard, A., Fernandez, E., Elvira, C., San Roman, J., and Planell, J.A. Mechanical and rheological improvement of a calcium phosphate cement by the addition of a polymeric drug. J Biomed Mater Res **57,** 113, 2001.
54. Xu, H.H., and Quinn, J.B. Calcium phosphate cement containing resorbable fibers for short-term reinforcement and macroporosity. Biomaterials **23,** 193, 2002.
55. Xu, H.H., Takagi, S., Quinn, J.B., and Chow, L.C. Fast-setting calcium phosphate scaffolds with tailored macropore formation rates for bone regeneration. J Biomed Mater Res Part A **68,** 725, 2004.
56. Xu, H.H., Eichmiller, F.C., and Giuseppetti, A.A. Reinforcement of a self-setting calcium phosphate cement with different fibers. J Biomed Mater Res **52,** 107, 2000.
57. Franceschi, R.T., Yang, S., Rutherford, R.B., Krebsbach, P.H., Zhao, M., and Wang, D. Gene therapy approaches for bone regeneration. Cells Tissues Organs **176,** 95, 2004.
58. Yang, S., Wei, D., Wang, D., Phimphilai, M., Krebsbach, P.H., and Franceschi, R.T. *In vitro* and *in vivo* synergistic interactions between the Runx2/Cbfa1 transcription factor and bone morphogenetic protein-2 in stimulating osteoblast differentiation. J Bone Miner Res **18,** 705, 2003.
59. Schneider, G.B., Whitson, S.W., and Cooper, L.F. Restricted and coordinated expression of beta3-integrin and bone sialoprotein during cultured osteoblast differentiation. Bone **24,** 321, 1999.
60. Yang, S., and Li, Y.P. RGS10-null mutation impairs osteoclast differentiation resulting from the loss of [Ca2+]i oscillation regulation. Genes Dev **21,** 1803, 2007.
61. Barzilay, R., Sadan, O., Melamed, E., and Offen, D. Comparative characterization of bone marrow-derived mesenchymal stromal cells from four different rat strains. Cytotherapy **11,** 435, 2009.
62. Harting, M., Jimenez, F., Pati, S., Baumgartner, J., and Cox, C., Jr. Immunophenotype characterization of rat mesenchymal stromal cells. Cytotherapy **10,** 243, 2008.
63. McCarty, R.C., Gronthos, S., Zannettino, A.C., Foster, B.K., and Xian, C.J. Characterisation and developmental potential of ovine bone marrow derived mesenchymal stem cells. J Cell Physiol **219,** 324, 2009.
64. Ruggeri, Z.M. von Willebrand factor. J Clin Invest **100,** S41, 1997.
65. Vailhe, B., Dietl, J., Kapp, M., Toth, B., and Arck, P. Increased blood vessel density in decidua parietalis is associated with spontaneous human first trimester abortion. Hum Reprod **14,** 1628, 1999.
66. Reddy, S., Wasnik, S., Guha, A., Kumar, J.M., Sinha, A., and Singh, S. Evaluation of nano-biphasic calcium phosphate ceramics for bone tissue engineering applications: *in vitro* and preliminary *in vivo* studies. J Biomater Appl 2012. DOI: 10.1177/0885328211415132
67. Moreau, J.L., and Xu, H.H. Mesenchymal stem cell proliferation and differentiation on an injectable calcium phosphate-chitosan composite scaffold. Biomaterials **30,** 2675, 2009.
68. Nan, K., Sun, S., Li, Y., Chen, H., Wu, T., and Lu, F. Ectopic osteogenic ability of calcium phosphate scaffolds cultured with osteoblasts. J Biomed Mater Res A **93,** 464, 2010.
69. Yuan, H., van Blitterswijk, C.A., de Groot, K., and de Bruijn, J.D. Cross-species comparison of ectopic bone formation in biphasic calcium phosphate (BCP) and hydroxyapatite (HA) scaffolds. Tissue Eng **12,** 1607, 2006.
70. Hollinger, J.O., and Battistone, G.C. Biodegradable bone repair materials. Synthetic polymers and ceramics. Clin Orthop Relat Res 290, 1986.
71. Garg, T., Singh, O., Arora, S., and Murthy, R. Scaffold: a novel carrier for cell and drug delivery. Crit Rev Ther Drug Carrier Syst **29,** 1, 2012.
72. Yamada, Y., Ueda, M., Naiki, T., Takahashi, M., Hata, K., and Nagasaka, T. Autogenous injectable bone for regeneration with mesenchymal stem cells and platelet-rich plasma: tissue-engineered bone regeneration. Tissue Eng **10,** 955, 2004.
73. Orsini, M., Orsini, G., Benlloch, D., Aranda, J.J., Lazaro, P., Sanz, M., *et al.* Comparison of calcium sulfate and autogenous bone graft to bioabsorbable membranes plus autogenous bone graft in the treatment of intrabony periodontal defects: a split-mouth study. J Periodontol **72,** 296, 2001.
74. Bron, J.L., Vonk, L.A., Smit, T.H., and Koenderink, G.H. Engineering alginate for intervertebral disc repair. J Mech Behav Biomed Mater **4,** 1196, 2011.

75. Park, D.J., Choi, B.H., Zhu, S.J., Huh, J.Y., Kim, B.Y., and Lee, S.H. Injectable bone using chitosan-alginate gel/mesenchymal stem cells/BMP-2 composites. J Craniomaxillofac Surg **33,** 50, 2005.
76. Zhao, L., Weir, M.D., and Xu, H.H. An injectable calcium phosphate-alginate hydrogel-umbilical cord mesenchymal stem cell paste for bone tissue engineering. Biomaterials **31,** 6502, 2010.
77. Bohari, S.P., Hukins, D.W., and Grover, L.M. Effect of calcium alginate concentration on viability and proliferation of encapsulated fibroblasts. Biomed Mater Eng **21,** 159, 2011.
78. Gaetani, R., Doevendans, P.A., Metz, C.H., Alblas, J., Messina, E., Giacomello, A., *et al.* Cardiac tissue engineering using tissue printing technology and human cardiac progenitor cells. Biomaterials **33,** 1782, 2012.
79. Itala, A.I., Ylanen, H.O., Ekholm, C., Karlsson, K.H., and Aro, H.T. Pore diameter of more than 100 microm is not requisite for bone ingrowth in rabbits. J Biomed Mater Res **58,** 679, 2001.
80. Schliephake, H., Neukam, F.W., and Klosa, D. Influence of pore dimensions on bone ingrowth into porous hydroxylapatite blocks used as bone graft substitutes. A histometric study. Int J Oral Maxillofac Surg **20,** 53, 1991.
81. Harris, W.H., and Jasty, M. Bone ingrowth into porous coated canine acetabular replacements: the effect of pore size, apposition, and dislocation. Hip 214, 1985.
82. Martens, M., Ducheyne, P., De Meester, P., and Mulier, J.C. Skeletal fixation of implants by bone ingrowth into surface pores. Arch Orthop Trauma Surg **97,** 111, 1980.
83. Hulbert, S.F., Young, F.A., Mathews, R.S., Klawitter, J.J., Talbert, C.D., and Stelling, F.H. Potential of ceramic materials as permanently implantable skeletal prostheses. J Biomed Mater Res **4,** 433, 1970.
84. Bobyn, J.D., Pilliar, R.M., Cameron, H.U., and Weatherly, G.C. The optimum pore size for the fixation of porous-surfaced metal implants by the ingrowth of bone. Clin Orthop Relat Res 263, 1980.
85. Wang, E.A., Rosen, V., D'Alessandro, J.S., Bauduy, M., Cordes, P., Harada, T., *et al.* Recombinant human bone morphogenetic protein induces bone formation. Proc Natl Acad Sci U S A **87,** 2220, 1990.
86. Sandhu, H.S. Bone morphogenetic proteins and spinal surgery. Spine (Phila Pa 1976) **28,** S64, 2003.
87. Khan, S.N., and Lane, J.M. The use of recombinant human bone morphogenetic protein-2 (rhBMP-2) in orthopaedic applications. Expert Opin Biol Ther **4,** 741, 2004.
88. Vaidya, R., Carp, J., Sethi, A., Bartol, S., Craig, J., and Les, C.M. Complications of anterior cervical discectomy and fusion using recombinant human bone morphogenetic protein-2. Eur Spine J **16,** 1257, 2007.
89. Marson, A.G., Hutton, J.L., Leach, J.P., Castillo, S., Schmidt, D., White, S., *et al.* Levetiracetam, oxcarbazepine, remacemide and zonisamide for drug resistant localization-related epilepsy: a systematic review. Epilepsy Res **46,** 259, 2001.
90. Steinert, A.F., Palmer, G.D., Pilapil, C., Noth, U., Evans, C.H., and Ghivizzani, S.C. Enhanced *in vitro* chondrogenesis of primary mesenchymal stem cells by combined gene transfer. Tissue Eng Part A **15,** 1127, 2009.
91. Castro-Govea, Y., Cervantes-Kardasch, V.H., Borrego-Soto, G., Martinez-Rodriguez, H.G., Espinoza-Juarez, M., Romero-Diaz, V., *et al.* Human bone morphogenetic protein 2-transduced mesenchymal stem cells improve bone regeneration in a model of mandible distraction surgery. J Craniofac Surg **23,** 392, 2012.
92. Sweeney, T.M., Opperman, L.A., Persing, J.A., and Ogle, R.C. Repair of critical size rat calvarial defects using extracellular matrix protein gels. J Neurosurg **83,** 710, 1995.
93. Rai, B., Oest, M.E., Dupont, K.M., Ho, K.H., Teoh, S.H., and Guldberg, R.E. Combination of platelet-rich plasma with polycaprolactone-tricalcium phosphate scaffolds for segmental bone defect repair. J Biomed Mater Res A **81,** 888, 2007.
94. Li, Z.H., Liao, W., Cui, X.L., Zhao, Q., Liu, M., Chen, Y.H., *et al.* Intravenous transplantation of allogeneic bone marrow mesenchymal stem cells and its directional migration to the necrotic femoral head. Int J Med Sci **8,** 74, 2011.
95. Saito, T., Kuang, J.Q., Bittira, B., Al-Khaldi, A., and Chiu, R.C. Xenotransplant cardiac chimera: immune tolerance of adult stem cells. Ann Thorac Surg **74,** 19; discussion 24, 2002.
96. Devine, S.M., Cobbs, C., Jennings, M., Bartholomew, A., and Hoffman, R. Mesenchymal stem cells distribute to a wide range of tissues following systemic infusion into nonhuman primates. Blood **101,** 2999, 2003.
97. Inoue, S., Popp, F.C., Koehl, G.E., Piso, P., Schlitt, H.J., Geissler, E.K., *et al.* Immunomodulatory effects of mesenchymal stem cells in a rat organ transplant model. Transplantation **81,** 1589, 2006.
98. Suwa, F., Fang, Y.R., Toda, I., Tang, C.S., Yang, L.J., Gao, Y.H., *et al.* SEM study on microvascular changes following implantation of bone morphogenetic protein combined with hydroxyapatite into experimental bone defects. J Osaka Dent Univ **32,** 27, 1998.
99. Deckers, M.M., van Bezooijen, R.L., van der Horst, G., Hoogendam, J., van Der Bent, C., Papapoulos, S.E., *et al.* Bone morphogenetic proteins stimulate angiogenesis through osteoblast-derived vascular endothelial growth factor A. Endocrinology **143,** 1545, 2002.

Address correspondence to:
Shuying Yang, MD, PhD
Department of Oral Biology
The State University of New York at Buffalo
36 Foster Hall, 3435 Main Street
Buffalo, NY 14214

E-mail: sy47@buffalo.edu

Received: April 15, 2012
Accepted: September 18, 2012
Online Publication Date: November 16, 2012